Title

Manipulating DNA damage-response signaling for the treatment of immune-mediated diseases

Journal

Proceedings of the National Academy of Sciences of the United States of America, 114(24)

ISSN

0027-8424

Authors

McNally, Jonathan P
Millen, Scott H
Chaturvedi, Vandana
et al.

Publication Date

2017-06-13

DOI

10.1073/pnas.1703683114

Peer reviewed

Manipulating DNA damage-response signaling for the treatment of immune-mediated diseases

Jonathan P. McNally[a,1], Scott H. Millen[a,1], Vandana Chaturvedi[a], Nora Lakes[a], Catherine E. Terrell[a], Eileen E. Elfers[a], Kaitlin R. Carroll[a], Simon P. Hogan[b], Paul R. Andreassen[c], Julie Kanter[d], Carl E. Allen[e], Michael M. Henry[f], Jay N. Greenberg[g], Stephan Ladisch[g], Michelle L. Hermiston[h], Michael Joyce[i], David A. Hildeman[a], Jonathan D. Katz[a,j,2], and Michael B. Jordan[a,k,2]

[a]Division of Immunobiology, Department of Pediatrics, Cincinnati Children's Medical Center and University of Cincinnati College of Medicine, Cincinnati, OH 45229; [b]Division of Allergy and Immunology, Department of Pediatrics, Cincinnati Children's Medical Center and University of Cincinnati College of Medicine, Cincinnati, OH 45229; [c]Division of Experimental Hematology and Cancer Biology, Department of Pediatrics, Cincinnati Children's Medical Center and University of Cincinnati College of Medicine, Cincinnati, OH 45229; [d]Department of Hematology and Oncology, Medical University of South Carolina, Charleston, SC 29425; [e]Section of Hematology/Oncology, Department of Pediatrics, Baylor College of Medicine, Houston, TX 77030; [f]Department of Hematology and Oncology, Phoenix Children's Hospital, Phoenix, AZ 85016; [g]Department of Hematology, Children's National Medical Center, Washington, DC 20010; [h]Department of Pediatrics, University of California, San Francisco School of Medicine, San Francisco, CA 94143; [i]Department of Hematology and Oncology, Nemours Children's Specialty Care, Jacksonville, FL 32258; [j]Division of Endocrinology, Diabetes Research Center, Department of Pediatrics, Cincinnati Children's Medical Center and University of Cincinnati College of Medicine, Cincinnati, OH 45229; and [k]Division of Bone Marrow Transplantation and Immune Deficiency, Department of Pediatrics, Cincinnati Children's Medical Center and University of Cincinnati College of Medicine, Cincinnati, OH 45229

Edited by Christopher C. Goodnow, The Garvan Institute of Medical Research, Darlinghurst, NSW, Australia, and approved April 27, 2017 (received for review March 13, 2017)

Antigen-activated lymphocytes undergo extraordinarily rapid cell division in the course of immune responses. We hypothesized that this unique aspect of lymphocyte biology leads to unusual genomic stress in recently antigen-activated lymphocytes and that targeted manipulation of DNA damage-response (DDR) signaling pathways would allow for selective therapeutic targeting of pathological T cells in disease contexts. Consistent with these hypotheses, we found that activated mouse and human T cells display a pronounced DDR in vitro and in vivo. Upon screening a variety of small-molecule compounds, we found that potentiation of p53 (via inhibition of MDM2) or impairment of cell cycle checkpoints (via inhibition of CHK1/2 or WEE1) led to the selective elimination of activated, pathological T cells in vivo. The combination of these strategies [which we termed "p53 potentiation with checkpoint abrogation" (PPCA)] displayed therapeutic benefits in preclinical disease models of hemophagocytic lymphohistiocytosis and multiple sclerosis, which are driven by foreign antigens or self-antigens, respectively. PPCA therapy targeted pathological T cells but did not compromise naive, regulatory, or quiescent memory T-cell pools, and had a modest nonimmune toxicity profile. Thus, PPCA is a therapeutic modality for selective, antigen-specific immune modulation with significant translational potential for diverse immune-mediated diseases.

autoimmunity | immune regulation | DNA damage response | therapeutics

The immune system has evolved under intense pressure from pathogens that proliferate very rapidly (1). In responding to infections, the adaptive immune system needs to mobilize rare pathogen-specific lymphocytes quickly. This mobilization is achieved by rapid, exponential expansion of responding lymphocyte clones. Indeed, antigen-activated T and B cells appear to have some of the most rapid division rates among all mammalian cell types (2). We hypothesized that this unique aspect of lymphocyte biology would cause significant genomic stress in responding lymphocytes and that novel forms of therapeutic immune suppression could be developed by exploiting this weakness. Such strategies would allow for "developmental" or "kinetic" targeting of pathological immune responses at the time of disease activity or organ rejection and could complement or replace chronic suppression of immune signaling or cytokine pathways. The recent preclinical and clinical development of a wide array of rationally designed small-molecule inhibitors of various signaling and effector molecules within DNA damage-response (DDR) cascades has provided an opportunity to test this hypothesis (3, 4).

We first looked for evidence of a DDR occurring in activated T cells in physiological contexts and found a broad DDR in murine and human T cells. Next, upon screening an array of DNA-damaging agents and DDR-altering small molecules for their ability to kill activated, but not resting, T cells, we identified two promising strategies. We found that inhibition of MDM2 (an endogenous inhibitor of p53) and inhibitors of cell cycle checkpoint kinases such as CHK1 or WEE1 (5, 6) displayed significant potency and selectivity in vitro and in vivo. Both strategies displayed synergy with a DNA-damaging drug or with each other. Furthermore, this combination of DDR-active drugs, which we term "p53 potentiation with checkpoint abrogation" (PPCA), proved to be highly efficacious in two diverse mouse models of human diseases, hemophagocytic lymphohistiocytosis (HLH)

Significance

Therapeutic immune suppression is essential for treating a variety of immune conditions, including autoimmune diseases, immunoregulatory disorders, and in transplantation. Reliance on broadly acting drugs carries substantial risks, and even pathway-specific agents are problematic, because most immune pathways have essential functions. The ideal form of immune suppression would be antigen-specific, suppressing an undesired immune response but sparing all others. We describe a unique strategy for therapeutic immune suppression, relying on targeted manipulation of DNA damage-response signaling, that exploits unique aspects of lymphocyte biology. This approach allows for highly selective suppression of recently activated T cells, displays clear therapeutic benefits, and has less off-target toxicity than conventional DNA-damaging drugs.

Author contributions: J.P.M., S.H.M., V.C., N.L., C.E.T., K.R.C., S.P.H., P.R.A., D.A.H., J.D.K., and M.B.J. designed research; J.P.M., S.H.M., V.C., N.L., C.E.T., E.E.E., K.R.C., and M.B.J. performed research; J.K., C.E.A., M.M.H., J.N.G., S.L., M.L.H., M.J., and M.B.J. contributed new reagents/analytic tools; J.P.M., S.H.M., V.C., N.L., C.E.T., E.E.E., K.R.C., S.P.H., D.A.H., J.D.K., and M.B.J. analyzed data; and J.P.M., S.H.M., V.C., K.R.C., D.A.H., J.D.K., and M.B.J. wrote the paper.

Conflict of interest statement: M.B.J. is an inventor on a patent filing related to this work. The authors have no other conflicts to disclose.

This article is a PNAS Direct Submission.

[1]J.P.M. and S.H.M. contributed equally to this work.

[2]To whom correspondence may be addressed. Email: michael.jordan@cchmc.org or jonathan.katz@cchmc.org.

This article contains supporting information online at www.pnas.org/lookup/suppl/doi:10.1073/pnas.1703683114/-/DCSupplemental.

and multiple sclerosis (MS), with minimal effects on nonactivated T cells or nonimmune toxicity. Thus, targeted manipulation of the DDR during a pathological immune response may provide a highly effective, nontoxic, and antigen-selective means of clinical immune modulation.

Results

Activated Mouse T Cells Display a DDR in Physiological Contexts. Activated lymphocytes are among the most sensitive cells to irradiation or DNA-damaging chemotherapeutics (7), suggesting that they exist precariously at the edge of genotoxic death. This exquisite sensitivity of activated lymphocytes to DNA-damaging drugs has been exploited for years for therapeutic immune suppression with little mechanistic insight. However, we recently reported the efficacy of etoposide, a genotoxic topoisomerase inhibitor (8), for the selective elimination of pathogenic, activated T cells in both mouse HLH and experimental autoimmune encephalitis (EAE) (9, 10). While investigating the mechanism of T-cell killing by genotoxic agents, we found that in vitro antigen-activated T cells differed from resting T cells in that they displayed significant amounts of DNA breakage (Fig. 1*A*). Although T cells activated in vitro with lectins or phorbol esters have been shown to display evidence of a DDR (11), a similar phenomenon in primary T cells activated with antigen has not previously been reported. Using physiologically activated, purified T cells that were viable and nonapoptotic, as assessed by permeability and phosphatidylserine exposure, we found that activated (but not resting) T cells had nuclear foci of phosphoser139 H2AX (γH2AX), a classic indicator of a DDR (12, 13) (Fig. 1*B*). Next, we assessed DDR signaling in vivo by assessing adoptively transferred T-cell receptor (TCR) transgenic T cells specific for lymphocytic choriomeningitis virus (LCMV) in infected hosts. Comparing these antigen-activated transgenic T cells with nonactivated naive T cells ($CD44^{lo}$) from the same animals, we found that the activated cells had clearly elevated γH2AX, p-p53, p-ATM, and p-CHK2 (Fig. 1*C*). Thus, T cells responding to a viral infection manifested a profound DDR in vivo. Notably, this damage response was occurring without exposure to exogenous genotoxins and indicated that this DDR is a normal part of T-cell responses. Furthermore, it shows that targeted manipulation of this endogenous DDR could be sufficient to cause selective apoptosis of recently activated lymphocytes.

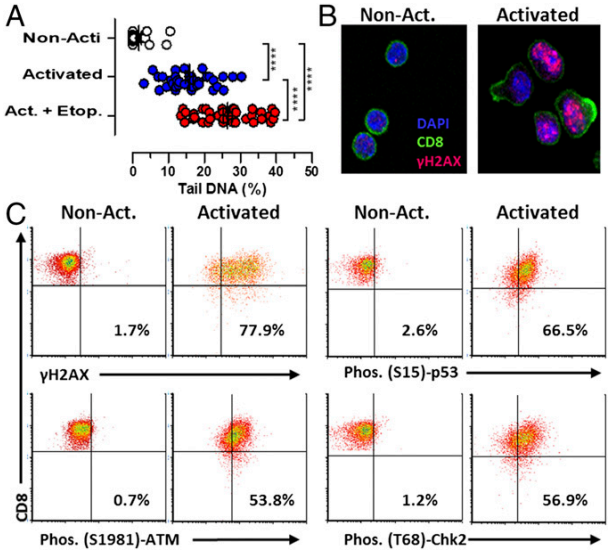

Fig. 1. Activated mouse T cells display a spontaneous DDR in physiological contexts. (*A*) Detection of DNA breaks in activated T cells via Comet Assay. Transgenic (P14) $CD8^+$ T cells were assayed either directly ex vivo [nonactivated (Non-Acti)] or after 5 d of in vitro activation and expansion with cognate peptide and IL-2. As a positive control, cells were cultured with etoposide (Etop., 1 μM) for 4 h. ****$P < 0.001$, determined by one-way ANOVA with a Bonferroni post hoc test. (*B*) Representative micrographs of nonactivated and activated T cells stained for γH2AX, a marker of the DDR. (Magnification, 40×.) (*C*) P14 T cells were transferred into recipient mice that were infected with LCMV on the following day. Six days after infection, splenic T cells were analyzed for the indicated intracellular phosphoproteins. Naive ($CD8^+$, $CD44^{lo}$) cells are compared with activated cells (transgenic; $CD8^+$, $CD45.1^+$) in the same animals. The percentages of cells in the upper right quadrant are shown. Results are representative of three independent experiments ($n = 8$ in *C*). Act., activated.

MDM2 Inhibition Synergizes with Etoposide for the Selective Killing of Activated T Cells. A large number of small-molecule agents targeting various aspects of the DDR and cell cycle regulation are currently in clinical and preclinical development for the treatment of cancer. We screened a panel of these agents for their ability to kill activated T cells in vitro, alone or in combination with etoposide. Although compounds inhibiting various proteins important for the DDR or cell cycle regulation [including ATM, DNA-PK, poly-ADP ribose polymerase, p53, polo-like kinase, aurora kinase, and various cyclin-dependent kinases] did not have significant activity in our assay, two strategies appeared promising: MDM2 inhibition and cell cycle checkpoint kinase inhibition (CHK1/2 or WEE1; see Fig. 3). MDM2 is an E3 ligase for p53 and drives its ubiquitin-mediated degradation (14). Thus, inhibition of MDM2 leads to increase of p53 levels and potentiation of its function in some contexts. It is known that p53 is a key regulator of cell fate decisions after DNA damage (15). Its initial activation leads to cell cycle arrest and attempts to repair the cellular damage that prompted its activation (16). However, if p53 signaling continues or there is an overwhelming amount of DNA damage, p53 drives apoptosis. A recent report describes MDM2 up-regulation and p53 down-regulation after T-cell activation, suggesting to us that this activity is an essential response to DNA damage associated with activation (17). Thus, we postulated that enhancement of p53 signaling would drive apoptosis of activated (but not resting) T cells. To test this hypothesis, we used the MDM2 inhibitor ($MDM2_i$) nutlin-3 (18). Although we did not observe significant effects of the $MDM2_i$ alone on survival of activated T cells, we found that MDM2 inhibition shifted the dose–response curve for etoposide-induced death of activated T cells in vitro (Fig. 2*A*). Mechanistically, we found that although MDM2 inhibition was not sufficient to induce phospho-p53 (Ser15) in activated T cells, it enhanced accumulation of phospho-p53 in etoposide-exposed cells (Fig. 2*B*). Furthermore, MDM2 inhibition did not increase γH2AX levels, a more proximal indicator of DNA damage (19), suggesting that it was amplifying the toxic effects of DNA breakage in these cells (Fig. 2*C*). As expected, $MDM2_i$ enhanced killing of activated T cells in a strictly p53-dependent manner (Fig. S1). Next, we assessed whether MDM2 inhibition could amplify the effects of etoposide on T cells in vivo. When we treated LCMV-infected mice with a subtherapeutic dose (fivefold less than a standard therapeutic dose) of etoposide, we found notable synergy with $MDM2_i$ (Fig. 2*D*). Although treatment with this low dose of etoposide had only a very modest effect on LCMV-activated cells (D^b-GP33 $tetramer^+$), the addition of $MDM2_i$ led to near-complete ablation of $tetramer^+$ (below the limit of detection) cells in these animals, in contrast to treatment with $MDM2_i$ alone. This effect was relatively selective, with a modest, albeit significant, effect of this combination on naive T cells (Fig. 2*E*). Thus, an $MDM2_i$ can synergize with DNA-damaging drugs for the selective elimination of recently activated T cells in vivo.

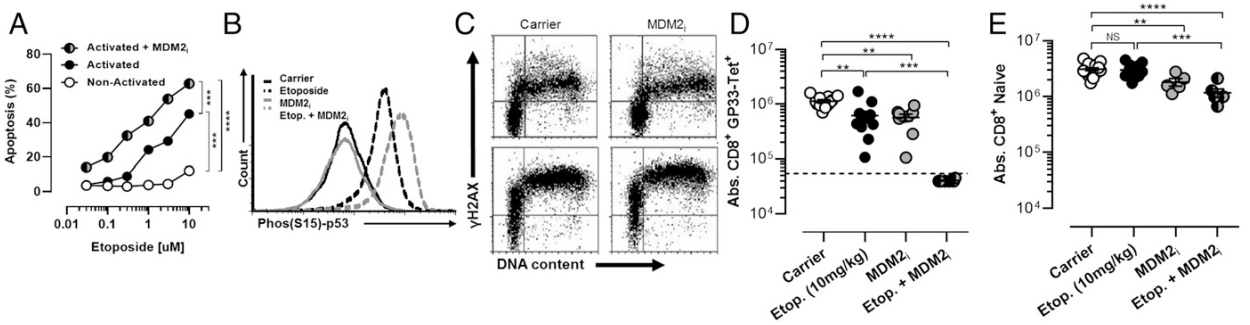

Fig. 2. MDM2 inhibition synergizes with etoposide for the selective killing of activated T cells. (*A*) Nonactivated or in vitro-activated CD8$^+$ T cells (P14, stimulated with peptide and then with IL-2 for 5 d) were cocultured with increasing concentrations of etoposide ± MDM2$_i$ and nutlin-3 (2.5 μM) for 18 h and assessed for apoptosis. (*B*) Phospho-p53 (Ser15) staining of activated T cells exposed to etoposide (1 μM) and/or MDM2$_i$ for 4 h. (*C*) γH2AX and DNA content (7-AAD) staining of activated T cells exposed to etoposide (1 μM) and/or MDM2$_i$ for 4 h. (*D* and *E*) WT mice were infected with LCMV and treated as indicated 5 d after infection. Etoposide was given at a subtherapeutic dose (10 mg/kg). Absolute numbers (Abs.) of splenic LCMV-specific (D^b-GP33 tetramer$^+$/CD44^{hi}) and naive (CD44^{lo}) CD8$^+$ T cells were enumerated 8 d after infection. Dotted lines represent the limit of tetramer detection. Data are mean (*A*) or individual animals (*C* and *D*) ± SE. Significance was determined by one-way ANOVA with a Bonferroni post hoc test. $^{**}P < 0.01$, $^{***}P < 0.001$, $^{****}P < 0.0001$. Results represent three independent experiments (n = 6–10).

Inhibition of Cell Cycle Checkpoint Kinases Selectively Kills Activated T Cells and Synergizes with Etoposide. When a cell senses DNA damage, progression through the cell cycle is halted to repair the DNA and allow for the survival of the cell. Cell cycle checkpoints may prevent either initiation of DNA replication (G_1/S) or progression at later phases of the cell cycle (mid-S or G_2/M). Although multiple mechanisms may enforce cell cycle checkpoints, p53 plays a dominant role in enforcing the G_1/S checkpoint via induction of p21^{cip} (20). For this reason, it has been speculated that p53-deficient malignant cells are highly dependent on the S and G_2/M checkpoints for maintaining their genomic integrity. Accordingly, a variety of kinase inhibitors have been developed as cancer therapeutics that inhibit CHK1, CHK2, or WEE1, the known enforcers of these later checkpoints (21, 22). We speculated that even though normal T cells have intact p53, their extraordinarily rapid rate of division would also make them exquisitely dependent on the S and G_2/M checkpoints for survival. Additionally, a recent report that T cells down-regulate p53 upon TCR stimulation also suggested to us that T cells may rely strongly on the S and G_2/M checkpoints (17). To test this hypothesis we used two different inhibitors of S and G_2/M cell cycle checkpoint proteins: the WEE1 inhibitor (WEE1$_i$) AZD1775 (23) and the CHK1/2 inhibitor (CHK$_i$) AZD7762 (24). Although the two compounds have distinct targets, they ultimately function by promoting premature S or G_2/M progression and initiation of mitosis.

When T cells were cultured with either compound, we observed a strong, dose-dependent proapoptotic effect, with substantial selectivity for activated over nonactivated T cells (Fig. 3*A*). Similar to the effects of MDM2$_i$, cotreatment with either CHK$_i$ or WEE1$_i$ shifted the etoposide dose–response curve for the killing of activated T cells (Fig. 3*B*). This enhanced killing appeared to be selective for activated T cells cycling at faster rates because these cells were more sensitive to treatment with CHK$_i$ or WEE1$_i$ (Fig. 3*C*). Furthermore, inhibition of cell cycle progression, via coinhibition of CDK2 (thus preventing entry from G_1 into S phase), provided substantial protection from CHK$_i$ or WEE1$_i$ exposure (Fig. 3*D*). Of note, CHK$_i$ treatment was equally effective in p53$^{-/-}$ and WT T cells, but MDM2 inhibition heightened this response only in WT T cells (Fig. S1). Careful cell cycle analysis of treated T cells using 5-ethynyl-2′-deoxyuridine incorporation and phospho-H3 staining (a marker of mitotic signaling) indicated that both CHK$_i$ and WEE1$_i$ led to an increase in the proportion of cells in G_2 and/or an increase in the proportion of cells that had initiated mitotic signaling (Fig. S2). Finally, when we assessed T cells after exposure to CHK$_i$ or WEE1$_i$, we found that cells in late S or G_2/M displayed a substantial increase in γH2AX levels and that those cells displaying premature mitotic signaling (those cells still in S-phase, but phospho-H3$^+$) had the highest levels (Fig. 3*E*). These results indicated that disturbing the mid-S and G_2/M checkpoints in activated T cells led to premature cell cycle progression, DNA damage, and death of these cells. They also suggested to us that CHK$_i$ or WEE1$_i$ would have substantial specificity in vivo for recently activated lymphocytes, which are transiting extremely rapidly through the cell cycle.

Next, we assessed the effects CHK$_i$ or WEE1$_i$ on activated T cells in vivo using an acute infection with LCMV. CHK$_i$ or WEE1$_i$ led to a significant loss of recently activated LCMV-specific (D^b-GP33 tetramer$^+$) T cells (Fig. 3*F*). This effect was relatively modest unless combined with a subtherapeutic dose of etoposide. However, when used in combination, there was a potent depletion of recently activated cells, with only a mild or moderate decrease of naive T cells (Fig. 3 *F* and *G*). Thus, CHK$_i$ and WEE1$_i$ display selective, potent, and antigen-specific immunosuppressive effects in combination with etoposide. Furthermore, we hypothesized that because MDM2$_i$ and CHK$_i$/WEE1$_i$ act on distinct nodes within the DDR, they may display synergistic effects when used in combination, and may allow for antigen-selective therapeutic immune suppression without the use of nonspecifically DNA-damaging drugs.

Combination Therapy with Inhibitors of MDM2 and Cell Cycle Checkpoint Kinases Selectively Eliminates Pathogenic CD8$^+$ T Cells, Suppresses Hypercytokinemia, and Treats Mouse HLH. HLH is a fatal immunoregulatory disorder affecting infants and children born with defects of perforin-dependent cytotoxic function (25). Because perforin-dependent cytotoxicity acts as a brake on T-cell activation, individuals with HLH display abnormally persistent and severe T-cell activation in response to infections or other stimuli. Conventional treatment of patients with HLH relies on etoposide, administered episodically (25). A well-established animal model involving LCMV infection of perforin-deficient (Prf$^{-/-}$) mice recreates this disorder and the therapeutic benefits of etoposide (10). However, because etoposide use is associated with significant adverse effects in clinical contexts, including marrow suppression and induction of secondary leukemia (26, 27), we tested an etoposide-free regimen in this model, relying solely on targeted manipulation of the DDR. We combined our previously identified strategies of MDM2 inhibition and CHK1/2 or WEE1 inhibition as a combination PPCA therapy. Administration of PPCA to LCMV-infected Prf$^{-/-}$ mice gave a synergistic effect, essentially

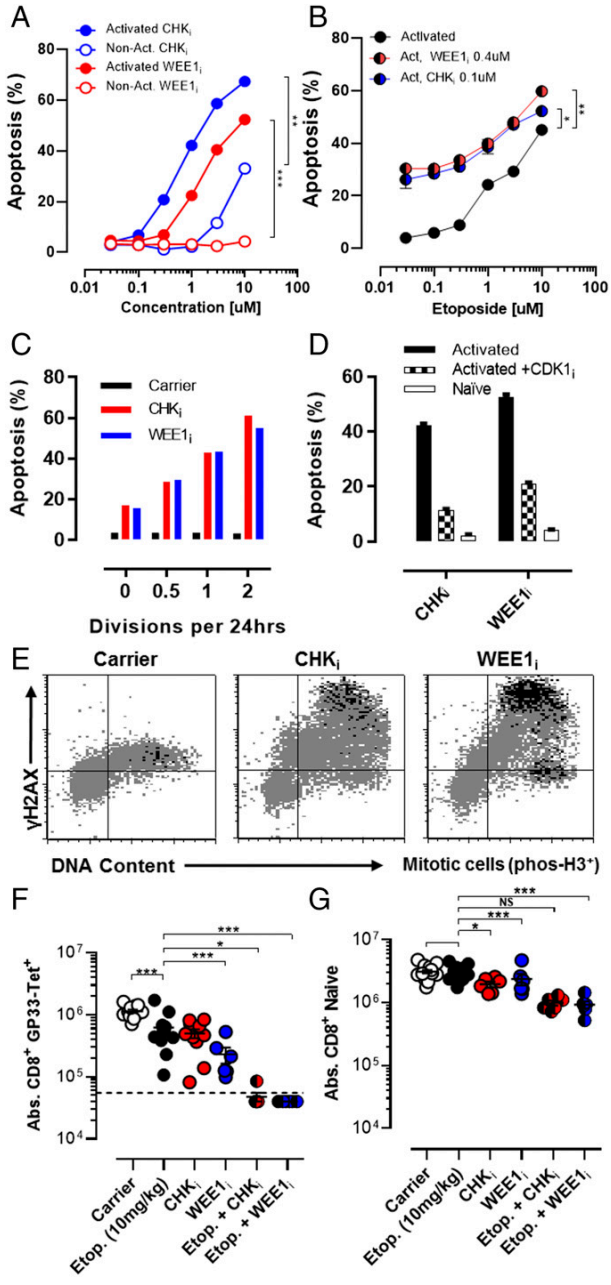

Fig. 3. Inhibition of cell cycle checkpoint kinases selectively kills activated T cells and synergizes with etoposide. (*A*) Nonactivated or in vitro-activated $CD8^+$ T cells (P14) were cocultured with increasing concentrations of either a CHK_i (AZD7762) or $WEE1_i$ (AZD1775) overnight and assessed for apoptosis. (*B*) Activated $CD8^+$ T cells (P14) were cocultured with increasing concentrations of etoposide ± a fixed concentration of either CHK_i or $WEE1_i$ for 18 h and assessed for apoptosis. (*C*) Activated $CD8^+$ T cells with a range of cell division rates (*Materials and Methods*) were cultured overnight with CHK_i, or $WEE1_i$ (1 or 10 μM) and assessed for apoptosis, which is plotted by division rates. (*D*) Activated $CD8^+$ T cells were cultured ± a selective CDK2 inhibitor (SU-9516, 5 μM), along with either CHK_i (1 μM) or $WEE1_i$ (10 μM), overnight and assessed for apoptosis. Nonactivated T cells exposed to these drugs are shown for comparison. (*E*) Representative flow plots of activated $CD8^+$ T cells cultured with either CHK_i (1μM) or $WEE1_i$ (10 μM) for 4 h, showing γH2AX expression, DNA content (7-AAD), and phospho-H3 (a marker of mitotic signaling). (*F* and *G*) WT mice were infected with LCMV and treated as indicated 5 d after infection. Etoposide was given at a subtherapeutic dose (10 mg/kg). Splenic LCMV-specific (D^b-GP33 $tetramer^+/CD44^{hi}$) and naive ($CD44^{lo}$) $CD8^+$ T cells were enumerated on day 8 postinfection. Data are mean (*A*–*D*) or individual animals (*F* and *G*) ± SE. Significance was determined by one-way ANOVA with a Bonferroni post hoc test. $^{**}P < 0.01$, $^{***}P < 0.001$. NS, not significant. Results represent three independent experiments ($n = 6$–12).

ablating the pathogenic anti-LCMV responses but largely sparing naive T cells, in contrast to the moderate loss of naive T cells seen when the inhibitors were used in combination with etoposide (Fig. 4 *A* and *B*). Next, we assessed systemic IFN-γ levels, a major mediator of HLH pathology (28, 29). PPCA gave efficient suppression of IFN-γ levels (Fig. 4*C*). Finally, we treated LCMV-infected $Prf^{-/-}$ mice with PPCA, incorporating either a CHK_i or $WEE1_i$, and found that whereas all mice treated with carrier died by about 3 wk after infection, most animals treated with PPCA survived long term (Fig. 4*D*). The efficacy of PPCA suggested that it may have significant potential for the clinical treatment of patients with HLH.

Combination PPCA Therapy Selectively Eliminates Pathogenic $CD4^+$ T Cells, Preserves Regulatory T Cells, and Treats EAE. To assess the wider applicability of PPCA to autoimmunity, we also tested it in the well-described model of MS, EAE, which is dependent on self-reactive $CD4^+$ T cells. EAE was induced in C57BL/6J mice with myelin oligodendrocyte glycoprotein (MOG)-derived peptide vaccination. Animals were treated with the combination of $WEE1_i$ and $MDM2_i$ (PPCA) on days 5 and 9 postimmunization. Splenic MOG-reactive $CD4^+$ T cells were analyzed on day 15 using either a tetrameric MHC peptide reagent ($I\text{-}A^b\text{-}MOG_{35–55}$ tetramer) or intracellular staining for IL-17A after MOG peptide stimulation. Both methodologies revealed a significant and similar decrease in MOG-reactive T cells after PPCA (Fig. 5 *A* and *B*), whereas naive $CD4^+$ T cells and regulatory T cells (Tregs) were spared (Fig. S3).

Although PPCA significantly decreased pathogenic $CD4^+$ T cells in vivo, we next needed to determine whether it would impact disease symptoms. PPCA therapy provided significant protection from the development of paralysis when given 5 and 9 d after initial vaccination (Fig. 5*C*), whereas treatment with $MDM2_i$ or $WEE1_i$ alone failed to provide disease protection (Fig. S3). The most stringent and clinically relevant test of therapy for EAE entails treatment after disease onset (30). In this context, we treated animals with clinically apparent disease on days 12 and 16, and observed significant protection from worsening paralysis, with a mean peak disease score of 1.9 vs. 2.6 (Fig. 5*D*). Thus, combination PPCA therapy selectively purges encephalitogenic $CD4^+$ T cells in EAE, sparing both naive $CD4^+$ T cells and Tregs, and displays therapeutic benefits in both preemptive and postparalysis therapeutic contexts.

Activated T Cells Are Uniquely Susceptible to DNA Damage Induction by Conventional Chemotherapeutics or PPCA Therapy, Although PPCA Spares Other Tissues. The therapeutic activity and immune selectivity we observed with PPCA suggested to us that activated effector T cells may be uniquely susceptible to DNA damage induction in vivo after exposure to DNA-modifying agents or targeted manipulation of the DDR, such as with PPCA. To investigate this idea, we examined DNA damage in various cell types directly ex vivo, using γH2AX staining. We compared activated $CD8^+$ T cells (as in Fig. 1), nonactivated $CD8^+$ T cells ($CD44^{lo}$), double-negative thymocytes, and lineage $(Lin)^-$/C-kit^+ (LK) marrow cells. At baseline, activated T cells had the highest γH2AX levels, followed by LK cells (Fig. 6*A*). Next, we compared γH2AX levels 2 h after animals were treated with etoposide, cyclophosphamide, or PPCA ($MDM2_i$ with either CHK_i or $WEE1_i$). Each of these approaches gave somewhat different γH2AX staining patterns, as illustrated by representative flow cytometric plots of

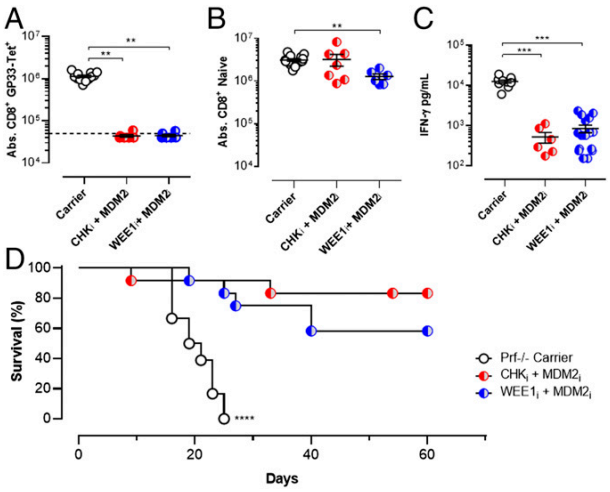

Fig. 4. PPCA selectively eliminates pathogenic CD8$^+$ T cells, suppresses hypercytokinemia, and treats mouse HLH. Prf$^{-/-}$ mice were infected with LCMV and treated as indicated on days 5 and 6 postinfection. (*A* and *B*) Splenic LCMV-specific (D^b-GP33 tetramer$^+$/CD44^{hi}) and naive (CD44^{lo}) CD8$^+$ T cells were enumerated on day 8 postinfection. (*C*) Serum IFN-γ levels from 8 d postinfection. (*D*) Survival of Prf$^{-/-}$ mice treated with drug carrier or indicated agents. Significance was determined by one-way ANOVA with a Bonferroni post hoc test. $^{**}P < 0.01$, $^{***}P < 0.001$. Results represent more than three independent experiments (n = 8–15 per group in *A*–*C*, *n* = 12–15 per group in *D*).

activated CD8$^+$ T cells in Fig. 6*B*. Etoposide gave the most profound increases, whereas cyclophosphamide and PPCA gave somewhat lower increases. Of note, γH2AX staining substantially underestimates the extent of DNA damage and the DDR in response to cyclophosphamide. This conventional chemotherapeutic acts by attaching alkyl groups to DNA and primarily causing intrastrand and interstrand cross-links. These cross-links are rapidly converted to DNA breaks in cells during S phase, but alkylation occurs at all phases of the cell cycle (and in nearly all cells). If not repaired, these lesions will lead to breakage at a later time points, during DNA replication or RNA transcription. Repair mechanisms for these lesions include base excision repair and other pathways that are not readily detectable by γH2AX staining.

When we compared the change in γH2AX staining 2 h after these treatments [normalized to the γH2AX mean fluorescent intensity (MFI) of the same cell type from carrier-treated animals], we observed that activated T cells experienced the most profound increases of all tissues assessed (Fig. 6*C*). Thus, activated effector T cells have the highest baseline DDR and are uniquely susceptible to further DNA damage induction by either DNA-damaging agents or targeted manipulation of DDR signaling pathways. This increased susceptibility, perhaps related to cell cycle speed (as in Fig. 3*C*), may be a primary mechanism underlying the efficacy of PPCA. Additionally, we noted that PPCA caused the smallest increase in γH2AX signal in all other cell types compared with etoposide or cyclophosphamide (Fig. 6*C* and Fig. S4). This observation demonstrates that PPCA has fewer off-target effects, and suggests that it may have substantially less toxicity, than conventional DNA-damaging drugs.

Combination Inhibitor Therapy Causes Minimal Off-Target Tissue Damage. Conventional chemotherapeutic agents damage DNA via a variety of biochemical mechanisms, including direct DNA binding/intercalation (alkylators, anthracyclines, and platinum derivatives), binding DNA-damaging intermediates (etoposide and camptothecins), or direct interference with DNA synthesis (e.g., methotrexate, cytarabine), and they usually do so in a tissue/cell-type nonspecific fashion. As such, the use of these agents for immune suppression is substantially limited by adverse effects, typically involving the gut and bone marrow. Because PPCA therapy relies instead on manipulating cell signaling downstream of endogenous DNA damage present in activated lymphocytes, we hypothesized that PPCA is less toxic than conventional chemotherapeutics.

We assessed potential gut, marrow, and immune toxicities of PPCA in experimental animals. As a functional assessment of gut toxicity, we measured small-molecule permeability (which rises with increasing gut damage) and transepithelial resistance (which falls with gut damage) of isolated terminal ileum from animals treated with PPCA or conventional chemotherapy (Fig. 7 *A* and *B*). Although the conventional DNA-damaging agents had a substantial impact on these measures of gut integrity, PPCA had a more modest or no impact.

Next, we examined the effects of combination PPCA therapy on hematopoietic progenitor cells. C-kit$^+$ progenitors [those progenitors positive for C-kit and negative for an array of Lin markers (LK cells)] are constantly dividing and are known to be some of the most sensitive cells to DNA-damaging agents. We compared the effects of conventional chemotherapy with the effects of PPCA and found that PPCA had a more limited effect on their numbers (Fig. 7*C*). Additionally, we examined the effects of these drugs on rapidly dividing double-negative thymocytes and found that PPCA caused less depletion than conventional agents (Fig. 7*D*). Thus, although PPCA therapy appears to rely (at least in part) on the uniquely rapid proliferative nature of activated lymphocytes, other proliferating cells types are spared by PPCA compared with conventional DNA-damaging agents. Importantly, this finding is consistent with published reports showing that MDM2$_i$, CHK1/2$_i$,

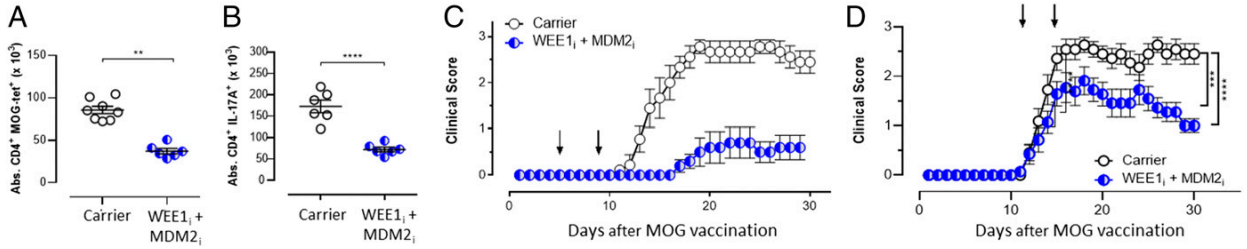

Fig. 5. PPCA selectively eliminates pathogenic CD4$^+$ T cells, preserves Tregs, and treats mouse EAE. C57BL/6 mice were vaccinated with MOG peptide to induce EAE and treated on days 5 and 9 after vaccination with drug carrier or PPCA. Splenocytes were harvested on day 30 and stained for MOG$_{35}$-specific CD4$^+$ T cells (CD4$^+$, CD44^{hi}, I-A^b MOG$_{35}$ tetramer$^+$) (*A*) and CD4$^+$ T cells producing IL-17 after ex vivo MOG$_{35–55}$ peptide stimulation (*B*). (*C*) MOG-vaccinated animals were treated on days 5 and 9 with combination inhibitor therapy and assessed for progressive paralysis using standard clinical scoring. (*D*) After the onset of paralysis, animals were treated as indicated (on days 12 and 16) and followed for clinical score. Data are mean ± SE. $^{**}P < 0.001$, $^{***}P < 0.001$, $^{****}P < 0.0005$. Results represent three independent experiments (*n* = 8–12).

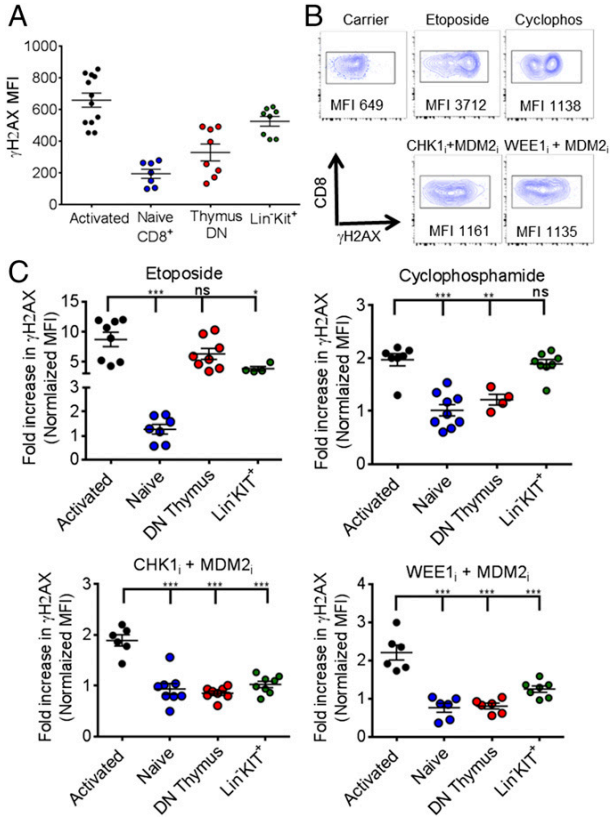

Fig. 6. Activated T cells are uniquely susceptible to DNA damage induction by conventional chemotherapeutics or PPCA, although PPCA spares other tissues. (*A*) γH2AX staining was assessed in various cell types directly ex vivo, including activated T cells (transferred CD45.1$^+$ P14 T cells, 6 d after LCMV infection), nonactivated CD8$^+$ T cells (CD44^{lo}), double-negative thymocytes, and LK marrow cells. (*B*) Representative flow cytometric plots, gating on LCMV-specific (CD8$^+$/CD45.1$^+$) splenic T cells, obtained 2 h after animals were treated with the indicated agents. Cyclos, cyclophosphamide. (*C*) Fold increase of γH2AX MFI (normalized to the same cell types from carrier-treated animals) of cells obtained 2 h after animals received the indicated treatments. Each symbol reflects data from individual mice, cumulative from two to three independent experiments. Mean ± SEM is shown. Differences between indicated groups were calculated using an unpaired Student's *t* test. *$P < 0.05$, **$P < 0.01$; ***$P < 0.001$. ns, not significant.

and WEE1$_i$ have demonstrated relatively mild toxicities in clinical trials (5, 31, 32).

Although PPCA therapy appears to spare nonactivated, bystander T cells, we wanted to look more closely at Tregs because they have been reported to be a chronically dividing T-cell population in vivo (33). Additionally, DNA-damaging agents, including cyclophosphamide, are reported to kill these cells (34, 35). To test the acute effects of combination PPCA therapy on Tregs, mice were treated twice with PPCA, cyclophosphamide, or etoposide, and total splenic Treg numbers were enumerated 1 d after the second treatment (Fig. 7*E*). Although cyclophosphamide treatment led to a substantial decrease in total Treg numbers, PPCA did not affect them.

Next, we tested whether quiescent memory T cells would be affected by exposure to PPCA. To generate a quiescent memory T-cell response under physiological conditions, we infected mice with LCMV (Armstrong) and waited 2 mo to establish a stable memory pool that slowly proliferates. Then, EAE was induced in the mice and in groups of mice that were treated with either PPCA or carrier. Twenty-one days after EAE induction, mice were rechallenged with LCMV clone 13 to assess the in vivo function of LCMV-specific memory T cells. As expected, rechallenge with LCMV caused a rapid increase in LCMV-specific CD8$^+$ T cells

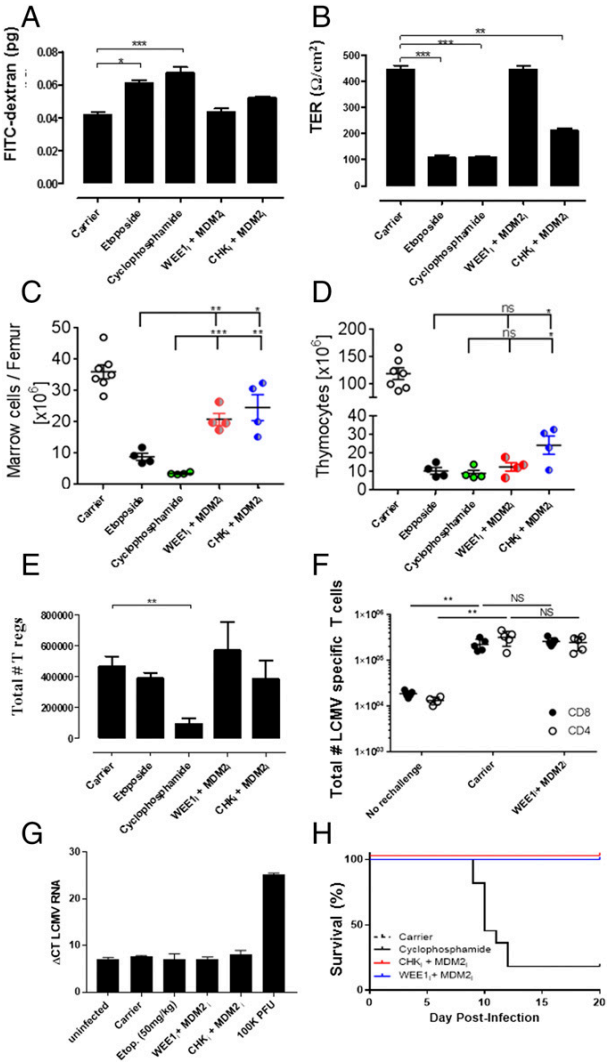

Fig. 7. PPCA causes minimal off-target tissue damage. For assessment of gut toxicity, WT mice were treated twice, as indicated, 24 h apart and tissues were harvested 24 h following the second treatment. FITC-dextran migration (*A*) and transepithelial resistance (*B*) were measured through isolated ileum using a Ussing chamber. Total cell counts from the bone marrow (one femur) (*C*) and thymus (*D*) of WT mice 3 d after treatment with indicated drugs are shown. (*E*) Total cell count per spleen of Tregs (CD4$^+$/CD25$^+$/FoxP3$^+$) 1 d after the indicated treatment. (*F*) WT mice were infected with LCMV (Armstrong), and EAE was induced and treated 60 d later, as per Fig. 5*E*. On day 81, mice were rechallenged with LCMV-CL13, and splenocytes were analyzed 5 d later for the total number of LCMV-specific D^b-GP33$^+$ memory CD8$^+$ T cells or IA^b-GP61$^+$ memory CD4$^+$ T cells by tetramer staining. "No rechallenge" indicates initial LCMV challenge but no further treatment or CL13 rechallenge. (*G*) WT mice were infected with LCMV and treated with the indicated agents, as per Fig. 4*D*. Seventy days later, spleens were assessed by quantitative PCR for persistence of virus. (*H*) WT BALB/c mice were infected with MCMV (Smith strain, 10^4 pfu), treated with the indicated drugs 3 d postinfection, and monitored for survival. Data are representative of two individual experiments with eight mice per group. Where indicated, data are mean ± SE. Significance was determined by one-way ANOVA with a Bonferroni post hoc test. *$P < 0.05$, **$P < 0.001$, ***$P < 0.001$. Results represent two to four independent experiments (n = 6–12). NS, not significant.

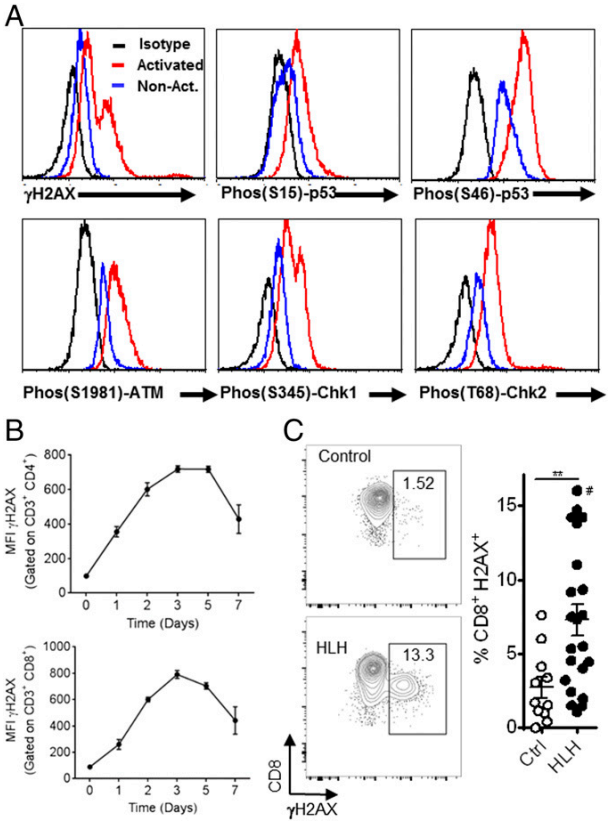

Fig. 8. Activated T cells from healthy human donors and peripheral blood T cells from patients with active HLH display a spontaneous DDR. (*A*) T cells from normal donors were activated in vitro (Con A, followed by IL-2) and assessed by flow cytometry for the indicated phosphoprotein markers, in comparison to nonactivated T cells. (*B*) Kinetics of γH2AX (MFI) expression in $CD4^+$ and $CD8^+$ T cells from human PBMCs after stimulation with anti-CD3 and anti-CD28 for 4 d and expansion in IL-2 for 3 d. Data are representative of three experiments with similar results. (*C*) PBMCs from healthy pediatric donors and patients with untreated, active HLH were assessed for the percentage of $\gamma H2AX^+$ cells among $CD3^+/CD8^+$ cells by flow cytometry. #, data point off scale at 32.1%. Data are mean ± SE. $^{**}P < 0.01$. Ctrl, control. Results represent three independent experiments (n = 12–27).

(D^b-GP33 tetramer$^+$), and the increases in these populations were unaffected by combination PPCA therapy given during EAE (Fig. 7*F*).

Finally, we asked whether PPCA would affect concurrent viral infections. We treated WT animals with PPCA on days 5 and 6 of LCMV infection (the same treatment and timing as for $Prf^{-/-}$ mice in Fig. 4). Seventy days later, mice were killed and spleens were assessed by quantitative PCR for the presence of LCMV. Despite treatment with PPCA or cyclophosphamide, all animals cleared the LCMV infection (Fig. 7*G*). Because even persistent LCMV may be nonpathogenic in WT animals (36), we sought to assess the effects of PPCA using a highly pathogenic virus, mouse cytomegalovirus (MCMV). Selgrade et al. (37) reported that when given early after MCMV infection, cyclophosphamide led to substantial mortality. We infected WT mice with MCMV, treated them with either PPCA or cyclophosphamide 3 d later, and observed that most cyclophosphamide mice died within 10 d, although no mice treated with PPCA or drug carrier died (Fig. 7*H*). Thus, taken together, PPCA potently suppresses recently activated T-cell responses, yet it has minimal or decreased off-target effects on the gut and marrow; it has limited off-target effects on bystander thymocytes, Tregs, and quiescent memory T cells; and it does not affect clearance or survival of concurrent viral infections, as demonstrated by two distinct viral infection models. These qualities indicate that PPCA has a superior toxicity profile compared with conventional DNA-damaging drugs currently used for immune modulation.

Activated T Cells from Healthy Human Donors and Peripheral Blood T Cells from Patients with Active HLH Display a Spontaneous DDR. The data above demonstrate that mouse T cells display a strong DDR when activated by antigen under physiological conditions. To understand the translational potential of this strategy better, we examined activated human T cells from healthy donors. T cells were activated and expanded in vitro with the lectin Con A, followed by IL-2, and examined via phosphospecific flow cytometry for various markers of the DDR. Similar to mouse T cells, we found that activated human T cells had elevated levels of γH2AX, phospho-p53, phospho-ATM, and phospho-CHK1/2 (Fig. 8*A*). To define the kinetics of this DDR, we stimulated normal donor lymphocytes with anti-CD3 and anti-CD28 for 4 d, followed by culture in IL-2 for 3 d, where we assessed γH2AX staining at the start of culture and regularly thereafter. We observed that both activated $CD4^+$ and $CD8^+$ T cells displayed an increase in γH2AX staining within 1 d of initial stimulation (Fig. 8*B*). The γH2AX levels increased further over the next few days as cells began to proliferate rapidly. Thus, initial activation and subsequent proliferation both contribute to the DDR in activated human T cells.

Because HLH is a disease of excessive T-cell activation, we postulated that we would be able to observe evidence of a DDR in T cells from patients with active disease, directly ex vivo and without stimulation. When we examined peripheral blood mononuclear cells (PBMCs) from patients with untreated HLH, we observed a significant increase in γH2AX in $CD8^+$ T cells compared with T cells from healthy donors (Fig. 8*C*). Thus, we found that human T cells, either activated in vitro or activated in vivo in the disease context of HLH, display clear evidence of a DDR.

Human T Cells Are Sensitive to MDM2, CHK1/2, and WEE1 Inhibition After Activation with Lectins or Specific Antigen. When we cultured T cells from healthy donors with titrations of etoposide, CHK_i, or $WEE1_i$, we found that Con A-activated, but not resting, T cells were very sensitive to each of these agents (Fig. 9 *A*–*C*). Furthermore, the addition of $MDM2_i$ to each of these agents enhanced killing of activated T cells. Of note, although the magnitude of killing was similar between activated human and mouse T cells, the selectivity of these agents for activated vs. nonactivated T cells was greater with human versus mouse cells. To assess the effect of PPCA on antigen-driven responses in humans, fluorescently labeled PBMCs were stimulated with a pool of human CMV peptides in culture and then treated with PPCA. Specific T-cell death was determined for activated (dye-diluted), resting memory ($CD45RA^-$), and naive ($CD45RA^+$) T-cell subsets (gating in Fig. S5) by comparing PPCA-treated with control cultures. PPCA induced high levels of cell death in antigen-activated T cells, although sparing both resting memory and naive human T cells (Fig. 9 *D*–*F*). Thus, human T cells display a similar or stronger pattern of DDR signaling with activation, sensitivity to DDR manipulation, and selectivity of these agents for activated T cells, as we observed with mouse T cells. These results suggest that the in vivo therapeutic activity we have observed in mice has significant translational potential for the treatment of human diseases.

Discussion

In the current study, we demonstrate that activated mouse and human T cells display a strong DDR with activation in physiological conditions and in the human disease context of HLH; they have a marked sensitivity to inhibition of MDM2, CHK1/2,

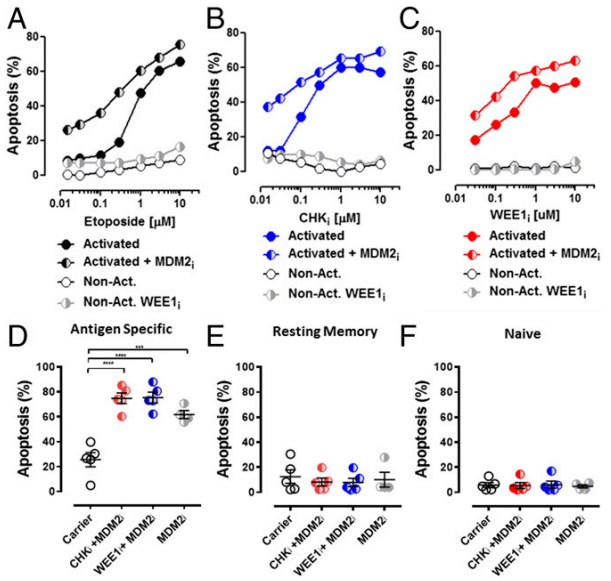

Fig. 9. Human T cells are sensitive to MDM2$_i$, CHK$_i$, and WEE1$_i$ after activation with lectins or specific antigen. Con A-activated and nonactivated T cells from healthy donors were cocultured with increasing concentrations of etoposide (*A*), CHK$_i$ (*B*), or WEE1$_i$ (*C*) ± MDM2$_i$ for 18 h and assessed for apoptosis. Separately, T cells were activated from healthy donor PBMCs with a CMV peptide pool followed by IL-2. Antigen-specific cells (*D*), resting memory cells (*E*), and naive T cells (*F*) were cultured with the indicated treatments (5 μM MDMD2$_i$, 3 μM etoposide, 1 μM CHK$_i$, and 1 μM WEE1$_i$), and apoptosis was assessed after 18 h. ***$P < 0.001$, ****$P < 0.0001$. Results represent five independent experiments.

or WEE1; and small-molecule agents targeting these proteins display significant potential for selective therapeutic immune suppression. The strategy of p53 potentiation (via MDM2$_i$) combined with inhibition of cell cycle checkpoint proteins (CHK1/2 or WEE1), termed PPCA therapy, allows for selective ablation of recently activated T cells, although sparing the naive, regulatory, and quiescent memory pools and evidencing minimal nonimmune toxicity. Moreover, PPCA appears to be broadly applicable, displaying clear benefits in models of a CD8$^+$ T-cell–driven immune regulatory disorder (HLH) and a CD4$^+$ T-cell–driven autoimmune disorder (EAE). Thus, this strategy represents a promising approach for the treatment of potentially many immune-mediated diseases.

Our findings represent a clear demonstration of DNA damage signaling in T cells responding to antigen in vivo or in vitro. We find that DNA damage is detectable once T cells are activated (at 24 h, before significant division; Fig. 8*B*), that T cells sustain greater damage than other cell types in response to PPCA or DNA-damaging agents (Fig. 6*C*), and that T cells dividing at faster rates are more sensitive to inhibition of CHK or WEE1 (Fig. 3*C*). Together, these observations suggest that extremely rapid cell division stresses cell cycle checkpoints to the limit of survivability and contributes to [but is likely not the only cause of (38)] DNA damage, which primes activated T cells for apoptosis. Thus, activated T cells, living near their DDR limits, are readily killed by additional DNA damage or by targeted inhibition of pathways critical for tolerance of their unusual biology. Further studies are needed to define more completely the critical pathways allowing lymphocytes to sustain their unique bursts of proliferation after activation.

The role of DDR signaling in the survival and function of mature T cells remains poorly defined. Multiple defects of the DDR, including mutations in ATM, ATR, DNA-PK, and other genes, are associated with immune deficiency (39). However, these mutations all cause severe abnormalities of lymphocyte development, and it is not clear to what extent peripheral T-cell function is altered. Indeed, the immune phenotypes of these disorders are similar to disorders of V(D)J recombination (e.g., RAG mutants), which is only active during the development of T cells. Of note, human diseases affecting multiple DNA repair pathways, including abnormalities of homologous and nonhomologous breakage repair, base excision repair, nucleotide excision repair, and repair of interstrand cross-links, are not associated with abnormal immune phenotypes (40). Furthermore, p53-deficient mice do not have an abnormal T-cell phenotype (41). Although multiple factors may limit peripheral T-cell expansion and survival (as in p53$^{-/-}$ mice), our findings suggest that proper function of specific DDR pathways is also critical for the survival of activated T cells.

Dozens of small-molecule inhibitors targeting DDR pathways have been developed, largely for the treatment of cancer (42). Multiple compounds have entered clinical trials, typically in combination with conventional chemotherapeutics as a way to enhance efficacy of DNA-damaging chemotherapy without promoting toxicity (43). Although clinical data are limited, initial experience suggests that these small-molecule drugs are well tolerated (44, 45). Although immune effects (or toxicities) of drugs that modulate DDR signaling have not been previously reported, our findings suggest that such effects should be examined in future clinical tests of DDR altering small molecules.

PPCA therapy is a novel combination. MDM2 was one of the first molecules targeted to manipulate DDR signaling (18). The normal function of MDM2 is to promote p53 degradation and limit its transcriptional activities and other functions (14). The normal function of CHK1 includes phosphorylation of CDC25, which induces S/G$_2$ arrest (24). Similarly, WEE1 functions to restrict mitotic entry by phosphorylating CDK1 and preventing its interaction with cyclin-B (46). Inhibition of these cell cycle checkpoint proteins leads to premature mitotic progression and is associated with heightened DDR signaling (Fig. 3). Because p53 activation potently enforces the G$_1$/S checkpoint, it has been theorized that p53-null tumors are especially dependent on the S and G$_2$/M checkpoints to maintain genomic integrity. Therefore, inhibitors of cell cycle checkpoint proteins have largely been developed for the treatment of p53-deficient malignancies (5, 21, 24, 47, 48). Meanwhile, MDM2$_i$s have been developed for use in p53-sufficient malignancies because they have little or no impact in the absence of p53. In theory, targeting of MDM2 may antagonize targeting of CHK1 or WEE1, because it may cause G$_1$ arrest. Indeed, Li et al. (49) report that MDM2$_i$ may protect p53 WT cells from WEE1 inhibition. However, we have not observed antagonism in vivo when assessing activated T cells, suggesting that the S and G$_2$/M checkpoints may be uniquely important for the survival of these cells. Thus, PPCA is unique not only because it is an unexpected and novel combination, but because it appears to exploit unique aspects of T-cell biology.

PPCA demonstrates reduced nonimmune toxicities compared with conventional DNA-damaging agents. Although DNA-damaging chemotherapeutics, such as etoposide and cyclophosphamide, may be highly effective immune suppressants, their clinical use is severely limited by adverse effects such as myelosuppression, gut toxicity, and induction of secondary malignancies (27, 50). In contrast, PPCA potentiates and amplifies endogenous genotoxic stresses in activated lymphocytes, although it causes minimal damage in other cell types (Fig. 6 and Fig. S4). Furthermore, because DDR-based therapy does not directly damage DNA and is not likely to affect cells that are not in cycle, it is relatively nongenotoxic to the recipient. In contrast to agents such as etoposide or cyclophosphamide, which damage DNA in essentially all cells (albeit more strongly in dividing ones) and throughout the cell cycle, PPCA relies on the unusual levels of DNA damage sustained by activated lymphocytes. Within the immune system, PPCA

spares Tregs and nonactivated naive or memory T cells, likely because they are either not dividing or divide much more slowly (2, 51). Thus, the high degree of susceptibility that activated lymphocytes display to PPCA, relative to other cell types, creates a favorable "therapeutic index," the ratio of potential therapeutic benefit to potential toxicity.

The efficiency of PPCA as a form of antigen-specific T-cell immune suppression raises questions regarding inadvertent suppression of immunity to incidental (or latent) viral infections in patients receiving PPCA therapy. Because our current report represents a proof of principle with favorable toxicity data, this issue will likely have to be resolved in empirical clinical studies. However, this risk appears quite low for several reasons. First, our studies (Fig. 7) demonstrate that PPCA does not impair functional bystander T-cell memory, prevent clearance of LCMV, or promote mortality after MCMV infection. Indeed, antiviral immunity in mice and humans appears to overshoot what is needed (52), so there is an ample margin of safety in most contexts. Second, PPCA is likely to be used transiently and episodically, given at times for maximal disease impact. Because PPCA would not be applied continuously (in contrast to strategies like cytokine blockade), it is far less likely to cause complications like latent tuberculosis reactivation, as seen with TNF blockade. Third, although treatment of immune disorders with conventional DNA-damaging chemotherapeutics is associated with increased risk of infection, this risk is mostly related to nonimmune effects on the marrow or gut, which PPCA minimizes. The experience of patients with HLH treated in international trials with etoposide demonstrates that most treatment-emergent infections are due to bacterial, not viral, infections largely secondary to myelosuppression (53). Finally, in contrast to the selective effects of PPCA, alternatives such as broad and nonspecific T-cell–depleting antibodies (e.g., antithymocyte globulin or alemtuzumab) are clearly associated with viral reactivation and disseminated viral and fungal infections (54). Thus, targeted manipulation of the DDR is likely to be superior to current therapeutic strategies in terms of infection risk.

As immune-based therapies become increasingly important for the future of anticancer therapies, it is equally fitting and intellectually satisfying to note that DDR-based strategies, rooted in cancer biology and developed for the treatment of malignancies, may find an important role in the treatment of immune-mediated disorders.

Materials and Methods

Mice. C57BL/6J, BALB/cJ, *C57BL/6-Prf1*^{tm1Sdz}*/J* (*Prf*$^{-/-}$), and B6.129S2-Trp53^{tm1Tyj}*/J* (*p53*$^{-/-}$) mice were purchased from The Jackson Laboratory and bred in-house. TCR-transgenic postnatal day (P) 14 mice [B6.Cg-Tcra^{tm1Mom} Tg(TcrLCMV)327Sdz] were a gift from P. Marrack (University of Colorado/Howard Hughes Medical Institute, Denver, CO). All mice were housed under specific pathogen-free conditions in an Association for Assessment and Accreditation of Laboratory Animal Care-approved barrier facility under the monitoring and care of the Cincinnati Children's Hospital Medical Center (CCHMC) veterinary staff. Experiments were performed with CCHMC Institutional Animal Care and Use Committee (IACUC) approval.

Viral Infections and Drug Treatments. LCMV viral stocks were grown in BHK-21 cells, and the number of plaque-forming units (pfu) was assayed on Vero cells as previously described (55). LCMV-WE was used in all studies (200 pfu administered i.p.), except the studies shown in Fig. 7 *F* and *G*, in which LCMV Armstrong (2×10^5 pfu administered i.p.) was used for initial challenge and mice were rechallenged with LCMV clone 13 (2×10^6 pfu administered i.v.). MCMV stocks were generated from salivary glands of Smith strain-infected animals and titered using standard plaque assays. BALB/c mice were infected i.p. with 1×10^4 pfu per animal. All chemotherapeutics were obtained from the Cincinnati Children's Hospital Medical Center clinical pharmacy or the indicated supplier, administered i.p., and dosed as follows: etoposide (10 or 50 mg/kg), cyclophosphamide (200 mg/kg), nutlin-3 (50 mg/kg; Cayman Chemicals), AZD1775 (60 mg/kg; Chemietek), and AZD6672 (25 mg/kg; Selleck Chemical).

HLH Induction. HLH was induced in Prf$^{-/-}$ mice by LCMV-WE infection as described elsewhere (29). Mice were examined longitudinally, typically three times per week, for development of HLH-like disease symptoms.

EAE Induction and Treatment. Female C57BL/6 mice were immunized s.c. with 100 μg of MOG_{35-55} emulsified in 5 mg/mL complete Freund's adjuvant (CFA) (Hooke Laboratories). On days 0 and 2, animals received i.p. injections of 250 ng of pertussis toxin (Hooke Laboratories). Disease severity was assessed every day thereafter and assigned a value using the following scale: 1, tail flaccidity; 2, hind-limb weakness; 3, hind-limb paralysis; 4, hind-limb and forelimb paralysis; 5, moribund.

Immunization and pertussis toxin injections were formulated to maximize the disease severity to be ≤3 per the manufacturer's specifications (Hooke Laboratories) and recommendations of our IACUC.

MHC Tetramer Staining and Flow Cytometry. Spleens from individual mice were harvested and crushed through a 70-μm cell strainer (BD Biosciences) to generate a single-cell suspension. A total of 2×10^6 cells were stained with different combinations of cell surface antibodies to CD4, CD8, CD44, CD62L, CD16/32, CD25, F4/80, and Foxp3 (purchased from Biolegend, eBiosciences, Miltenyi Biotec, or Rockland Immunochemicals). The MOG_{35-55} I-A^b, LCMV GP_{61-80} I-A^b, and LCMV GP_{33-41} D^b tetramers were provided by the NIH Tetramer Core. Phosphoprotein staining for γH2Ax, phos-p53, phos-ATM, and phos-CHK1 or phos-CHK2 was performed after fixation and permeabilization with either methanol or Foxp3 permeabilization buffer (Biolegend) using antibodies from Cell Signaling Technology. For all staining of human cells or staining of murine cells after in vitro culture or drug treatment, dead cells were excluded by fixable viability dye staining. For ex vivo assessment of γH2AX and other DDR phosphoproteins, spleens were disaggregated in 0.3% paraformaldehyde directly to prevent apoptotic loss of activated cells due to tissue disruption.

Ex Vivo Cytokine Production. T cells were assessed by restimulation with 5 μg of peptide, MOG_{35-55}, GP_{33-41}, or GP_{61-80} (Synthetic Biomolecules) in the presence of Golgi Plug (BD Biosciences). Cells were permeabilized using a Cytofix/Cytoperm Kit (BD Biosciences) and stained with anti–IFN-γ or anti–IL-17a (Biolegend). Where noted, $CD4^+$ T cells were isolated from spleen and inguinal lymph nodes and purified by negative selection using a $CD4^+$ T Cell Isolation Kit II (Miltenyi Biotec) before staining. Flow cytometry data were acquired on a FACSCaliber or LSR Fortessa (BD Biosciences) and were analyzed using FlowJo software version 7.6.5 (TreeStar, Inc.).

In Vitro Cell Death Assay. Splenocytes were harvested from P14 TCR transgenic mice, activated in vitro with the cognate peptide (LCMV GP_{33-41}, 1 μg/mL), and cultured in complete DMEM media for 2 d. Human T cells were enriched from PBMCs of normal healthy donors and stimulated with Con A (5 μg/mL), or whole PBMCs were stimulated with Pepmix CMV IE1 peptide pool (JTP). Activated human or mouse cells were then expanded in vitro with IL-2 (100 U/mL; PeproTech) for 3–5 d, except where noted otherwise. Nonactivated T cells were obtained by purifying $CD8^+$ cells from C57BL/6J spleens. For all assays, viable cells were purified by Ficoll (GE Life Sciences) gradient centrifugation before culturing with the indicated drug. Cells were cultured for 18 h with the indicated treatments, and apoptosis was evaluated by measuring phosphatidylserine exposure using A647-labeled MFG-E8 binding (56) and permeability using 7-AAD (Biolegend) or the viability dye eFluor 506 (eBiosciences). For all dose–response curves depicting cell killing by drugs, the death shown is the death measured above baseline (untreated cells), which was typically 10–15%.

Comet Assay. Naive and in vitro-activated P14 $CD8^+$ T cells were assessed for DNA damage per the manufacturer's recommendations for a neutral Comet Assay (Trevigen). In short, 1×10^5 T cells were mixed with 37 °C agarose plated on slides. Cells were lysed overnight and rinsed before electrophoresis. Slides were dried at 37 °C, stained with SYBR Gold, and viewed on a Leica ST-2 fluorescent microscope.

Tissue Processing for Toxicity Assessment. C57BL/6J cells were treated as described 24 h apart, and tissues were harvested 24 h later. Terminal ileum was harvested and assessed using a Ussing chamber as previously described (57).

Study Design. Human blood samples were obtained from healthy donors and patients with HLH under CCHMC Institutional Review Board-approved Protocols 2009-2797 and 2008-0483. Written informed consent was received

from participants before inclusion in the study. Animal experiments were performed with IACUC approval.

Statistics. Where appropriate, results are given as the mean ± SEM, with statistical significance determined by a two-tailed *t* test using either paired or unpaired (assuming equal variance) or one-way ANOVA with a Dunnett post hoc test, according to the data characteristics. Survival curves were assessed by the Wilcoxon–Gehan test for differences among groups. Significance was defined as $P < 0.05$. Statistical analysis was performed using GraphPad Prism 5.04 software (GraphPad Software, Inc.).

ACKNOWLEDGMENTS. We thank the Cincinnati Rheumatic Diseases Center Animal Models of Inflammatory Disease Core (NIH Grant P30 AR047363) at the CCHMC for help in setting up our EAE model. Additionally, we thank Simon Hogan and David Wu for assisting in the assessment of gastrointestinal permeability. We thank Rhonda Cardin for assistance with MCMV studies. We thank Harinder Singh for invaluable feedback on this manuscript. We also thank the NIH Tetramer Core for the MOG_{35-55} I-A^b, LCMV GP_{61-80} I-A^b, and LCMV GP_{33-41} D^b tetramers. This work was supported by NIH Grants RO1DK081175 (to J.D.K. and D.A.H.), RO1AI109810 (to M.B.J. and D.A.H.), and RO1AI057753 (to D.A.H.), as well by as a Research Innovation grant provided by the CCHMC (to M.B.J. and D.A.H.).

1. Pancer Z, Cooper MD (2006) The evolution of adaptive immunity. *Annu Rev Immunol* 24:497–518.
2. Yoon H, Kim TS, Braciale TJ (2010) The cell cycle time of CD8+ T cells responding in vivo is controlled by the type of antigenic stimulus. *PLoS One* 5:e15423.
3. Essmann F, Schulze-Osthoff K (2012) Translational approaches targeting the p53 pathway for anti-cancer therapy. *Br J Pharmacol* 165:328–344.
4. Kelley MR, Logsdon D, Fishel ML (2014) Targeting DNA repair pathways for cancer treatment: What's new? *Future Oncol* 10:1215–1237.
5. Seto T, et al. (2013) Phase I, dose-escalation study of AZD7762 alone and in combination with gemcitabine in Japanese patients with advanced solid tumours. *Cancer Chemother Pharmacol* 72:619–627.
6. Kreahling JM, et al. (2012) MK1775, a selective Wee1 inhibitor, shows single-agent antitumor activity against sarcoma cells. *Mol Cancer Ther* 11:174–182.
7. Heylmann D, Rödel F, Kindler T, Kaina B (2014) Radiation sensitivity of human and murine peripheral blood lymphocytes, stem and progenitor cells. *Biochim Biophys Acta* 1846:121–129.
8. Bromberg KD, Burgin AB, Osheroff N (2003) A two-drug model for etoposide action against human topoisomerase IIalpha. *J Biol Chem* 278:7406–7412.
9. McNally JP, et al. (2014) Eliminating encephalitogenic T cells without undermining protective immunity. *J Immunol* 192:73–83.
10. Johnson TS, et al. (2014) Etoposide selectively ablates activated T cells to control the immunoregulatory disorder hemophagocytic lymphohistiocytosis. *J Immunol* 192: 84–91.
11. Tanaka T, Kajstura M, Halicka HD, Traganos F, Darzynkiewicz Z (2007) Constitutive histone H2AX phosphorylation and ATM activation are strongly amplified during mitogenic stimulation of lymphocytes. *Cell Prolif* 40:1–13.
12. Banáth JP, Olive PL (2003) Expression of phosphorylated histone H2AX as a surrogate of cell killing by drugs that create DNA double-strand breaks. *Cancer Res* 63: 4347–4350.
13. Rogakou EP, Pilch DR, Orr AH, Ivanova VS, Bonner WM (1998) DNA double-stranded breaks induce histone H2AX phosphorylation on serine 139. *J Biol Chem* 273: 5858–5868.
14. Kruse J-P, Gu W (2009) Modes of p53 regulation. *Cell* 137:609–622.
15. Kracikova M, Akiri G, George A, Sachidanandam R, Aaronson SA (2013) A threshold mechanism mediates p53 cell fate decision between growth arrest and apoptosis. *Cell Death Differ* 20:576–588.
16. Topham CH, Taylor SS (2013) Mitosis and apoptosis: How is the balance set? *Curr Opin Cell Biol* 25:780–785.
17. Watanabe M, Moon KD, Vacchio MS, Hathcock KS, Hodes RJ (2014) Downmodulation of tumor suppressor p53 by T cell receptor signaling is critical for antigen-specific CD4(+) T cell responses. *Immunity* 40:681–691.
18. Vassilev LT, et al. (2004) In vivo activation of the p53 pathway by small-molecule antagonists of MDM2. *Science* 303:844–848.
19. Siliciano JD, et al. (1997) DNA damage induces phosphorylation of the amino terminus of p53. *Genes Dev* 11:3471–3481.
20. Szak ST, Mays D, Pietenpol JA (2001) Kinetics of p53 binding to promoter sites in vivo. *Mol Cell Biol* 21:3375–3386.
21. Landau HJ, et al. (2012) The checkpoint kinase inhibitor AZD7762 potentiates chemotherapy-induced apoptosis of p53-mutated multiple myeloma cells. *Mol Cancer Ther* 11:1781–1788.
22. Guertin AD, et al. (2013) Preclinical evaluation of the WEE1 inhibitor MK-1775 as single-agent anticancer therapy. *Mol Cancer Ther* 12:1442–1452.
23. Hirai H, et al. (2010) MK-1775, a small molecule Wee1 inhibitor, enhances anti-tumor efficacy of various DNA-damaging agents, including 5-fluorouracil. *Cancer Biol Ther* 9:514–522.
24. Zabludoff SD, et al. (2008) AZD7762, a novel checkpoint kinase inhibitor, drives checkpoint abrogation and potentiates DNA-targeted therapies. *Mol Cancer Ther* 7: 2955–2966.
25. Jordan MB, Allen CE, Weitzman S, Filipovich AH, McClain KL (2011) How I treat hemophagocytic lymphohistiocytosis. *Blood* 118:4041–4052.
26. My LT, et al. (2010) Comprehensive analyses and characterization of haemophagocytic lymphohistiocytosis in Vietnamese children. *Br J Haematol* 148:301–310.
27. Imashuku S (2007) Etoposide-related secondary acute myeloid leukemia (t-AML) in hemophagocytic lymphohistiocytosis. *Pediatr Blood Cancer* 48:121–123.
28. Zoller EE, et al. (2011) Hemophagocytosis causes a consumptive anemia of inflammation. *J Exp Med* 208:1203–1214.
29. Jordan MB, Hildeman D, Kappler J, Marrack P (2004) An animal model of hemophagocytic lymphohistiocytosis (HLH): CD8+ T cells and interferon gamma are essential for the disorder. *Blood* 104:735–743.
30. Constantinescu CS, Farooqi N, O'Brien K, Gran B (2011) Experimental autoimmune encephalomyelitis (EAE) as a model for multiple sclerosis (MS). *Br J Pharmacol* 164: 1079–1106.
31. Do K, et al. (2015) Phase I study of single-agent AZD1775 (MK-1775), a Wee1 kinase inhibitor, in patients with refractory solid tumors. *J Clin Oncol* 33:3409–3415.
32. Patnaik A, et al. (2015) Clinical pharmacology characterization of RG7112, an MDM2 antagonist, in patients with advanced solid tumors. *Cancer Chemother Pharmacol* 76:587–595.
33. Suffner J, et al. (2010) Dendritic cells support homeostatic expansion of Foxp3+ regulatory T cells in Foxp3.LuciDTR mice. *J Immunol* 184:1810–1820.
34. Brode S, Raine T, Zaccone P, Cooke A (2006) Cyclophosphamide-induced type-1 diabetes in the NOD mouse is associated with a reduction of CD4+CD25+Foxp3+ regulatory T cells. *J Immunol* 177:6603–6612.
35. Lutsiak MEC, et al. (2005) Inhibition of CD4(+)25+ T regulatory cell function implicated in enhanced immune response by low-dose cyclophosphamide. *Blood* 105: 2862–2868.
36. Oldstone MB (2013) Lessons learned and concepts formed from study of the pathogenesis of the two negative-strand viruses lymphocytic choriomeningitis and influenza. *Proc Natl Acad Sci USA* 110:4180–4183.
37. Selgrade MK, Daniels MJ, Hu PC, Miller FJ, Graham JA (1982) Effects of immunosuppression with cyclophosphamide on acute murine cytomegalovirus infection and virus-augmented natural killer cell activity. *Infect Immun* 38:1046–1055.
38. Huang X, Tanaka T, Kurose A, Traganos F, Darzynkiewicz Z (2006) Constitutive histone H2AX phosphorylation on Ser-139 in cells untreated by genotoxic agents is cell-cycle phase specific and attenuated by scavenging reactive oxygen species. *Int J Oncol* 29:495–501.
39. Slatter MA, Gennery AR (2010) Primary immunodeficiencies associated with DNA-repair disorders. *Expert Rev Mol Med* 12:e9.
40. O'Driscoll M (2012) Diseases associated with defective responses to DNA damage. *Cold Spring Harb Perspect Biol* 4:12.
41. Grayson JM, Lanier JG, Altman JD, Ahmed R (2001) The role of p53 in regulating antiviral T cell responses. *J Immunol* 167:1333–1337.
42. Hosoya N, Miyagawa K (2014) Targeting DNA damage response in cancer therapy. *Cancer Sci* 105:370–388.
43. Jackson SP, Helleday T (2016) DNA repair. Drugging DNA repair. *Science* 352: 1178–1179.
44. Bai L, Wang S (2014) Targeting apoptosis pathways for new cancer therapeutics. *Annu Rev Med* 65:139–155.
45. Wahl DR, Lawrence TS (2017) Integrating chemoradiation and molecularly targeted therapy. *Adv Drug Deliv Rev* 109:74–83.
46. Do K, Doroshow JH, Kummar S (2013) Wee1 kinase as a target for cancer therapy. *Cell Cycle* 12:3159–3164.
47. Hirai H, et al. (2009) Small-molecule inhibition of Wee1 kinase by MK-1775 selectively sensitizes p53-deficient tumor cells to DNA-damaging agents. *Mol Cancer Ther* 8: 2992–3000.
48. Ma Z, et al. (2012) The Chk1 inhibitor AZD7762 sensitises p53 mutant breast cancer cells to radiation in vitro and in vivo. *Mol Med Rep* 6:897–903.
49. Li Y, Saini P, Sriraman A, Dobbelstein M (2015) Mdm2 inhibition confers protection of p53-proficient cells from the cytotoxic effects of Wee1 inhibitors. *Oncotarget* 6: 32339–32352.
50. Bosca I, Pascual AM, Casanova B, Coret F, Sanz MA (2008) Four new cases of therapy-related acute promyelocytic leukemia after mitoxantrone. *Neurology* 71:457–458.
51. Walker LSK, Chodos A, Eggena M, Dooms H, Abbas AK (2003) Antigen-dependent proliferation of CD4+ CD25+ regulatory T cells in vivo. *J Exp Med* 198:249–258.
52. Wojciechowski S, et al. (2006) Bim mediates apoptosis of CD127(lo) effector T cells and limits T cell memory. *Eur J Immunol* 36:1694–1706.
53. Trottestam H, et al.; Histiocyte Society (2011) Chemoimmunotherapy for hemophagocytic lymphohistiocytosis: Long-term results of the HLH-94 treatment protocol. *Blood* 118:4577–4584.
54. Mahlaoui N, et al. (2007) Immunotherapy of familial hemophagocytic lymphohistiocytosis with antithymocyte globulins: A single-center retrospective report of 38 patients. *Pediatrics* 120:e622–e628.
55. Hildeman D, Yañez D, Pederson K, Havighurst T, Muller D (1997) Vaccination against persistent viral infection exacerbates CD4+ T-cell-mediated immunopathological disease. *J Virol* 71:9672–9678.
56. Bu HF, et al. (2007) Milk fat globule-EGF factor 8/lactadherin plays a crucial role in maintenance and repair of murine intestinal epithelium. *J Clin Invest* 117:3673–3683.
57. Wu D, et al. (2011) Interleukin-13 (IL-13)/IL-13 receptor alpha1 (IL-13Ralpha1) signaling regulates intestinal epithelial cystic fibrosis transmembrane conductance regulator channel-dependent Cl- secretion. *J Biol Chem* 286:13357–13369.

Supporting Information

McNally et al. 10.1073/pnas.1703683114

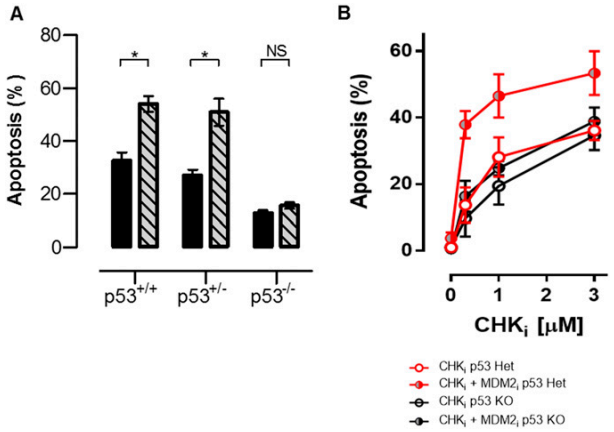

Fig. S1. MDM2 inhibition kills activated T cells in a p53-dependent fashion. (*A*) Activated [phytohemagglutinin (PHA)-stimulated] T cells from WT, $p53^{+/-}$, or $p53^{-/-}$ mice were cultured with etoposide (1 μM) or etoposide + $MDM2_i$ for 18 h and assessed for apoptosis. (*B*) Activated T cells from WT, $p53^{+/-}$, or $p53^{-/-}$ mice were cultured with CHK_i ± $MDM2_i$ for 18 h and assessed for apoptosis. Data are mean ± SE. Significance was determined by one-way ANOVA with a Bonferroni post hoc test. $*P < 0.05$. NS, not significant. Results represent three independent experiments. Het, heterozygous.

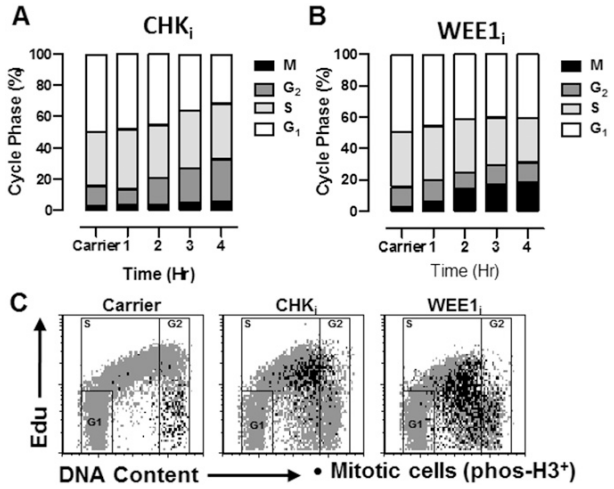

Fig. S2. Inhibitors of cell cycle checkpoint kinases promote premature cell cycle progression in activated T cells. Activated $CD8^+$ T cells were cultured with inhibitors of CHK_i or $WEE1_i$ for 4 h. 5-Ethynyl-2′-deoxyuridine (Edu) was added after 3 h, and cells were stained for Edu incorporation, DNA content (7-AAD), and phospho-H3 to define cell cycle status. Edu incorporation indicates S phase, phospho-H3 indicates M phase, and G_1 and G_2 are further defined by DNA content. (*A* and *B*) Quantitative assessment of cell cycle status. (*C*) Representative flow cytometric plots. Cells in G_1, S, and G_2 are represented in gray, with gates shown. Mitotic phospho-$H3^+$ cells are shown in black.

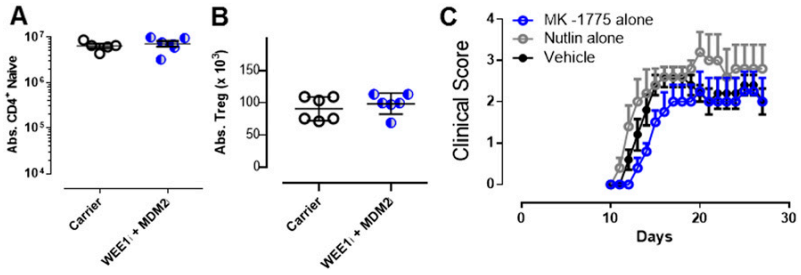

Fig. S3. Individual components of PPCA therapy are not effective in the treatment of EAE. C57BL/6 mice were vaccinated with MOG peptide to induce EAE and treated on days 5 and 9 after vaccination with drug carrier or PPCA. Splenocytes were harvested on day 30 and stained for naive $CD4^+$ T cells [*A*; absolute number (Abs.) of $CD44^{lo}$, $tetramer^-$] and Tregs (*B*; Abs. of $CD4^+$, $CD25^+$, $Foxp3^+$). (*C*) C57BL/6 mice were vaccinated with MOG peptide to induce EAE; treated on days 5 and 9 after vaccination with drug carrier, $WEE1_i$, or $MDM2_i$; and assessed for progressive paralysis using standard clinical scoring. Data are mean ± SE. Results represent three independent experiments (n = 8–12).

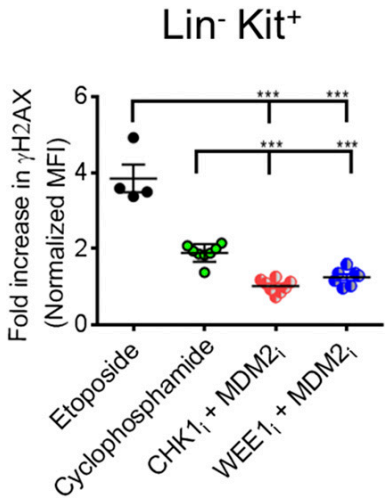

Fig. S4. PPCA therapy induces less DNA damage in marrow precursors. Cumulative data are shown comparing the MFI of gH2AX among LK cells in the bone marrow 2 h after animals received the indicated treatment. The MFI was normalized to carrier-treated mice. Data are individual animals with mean ± SEM. ***$P < 0.001$.

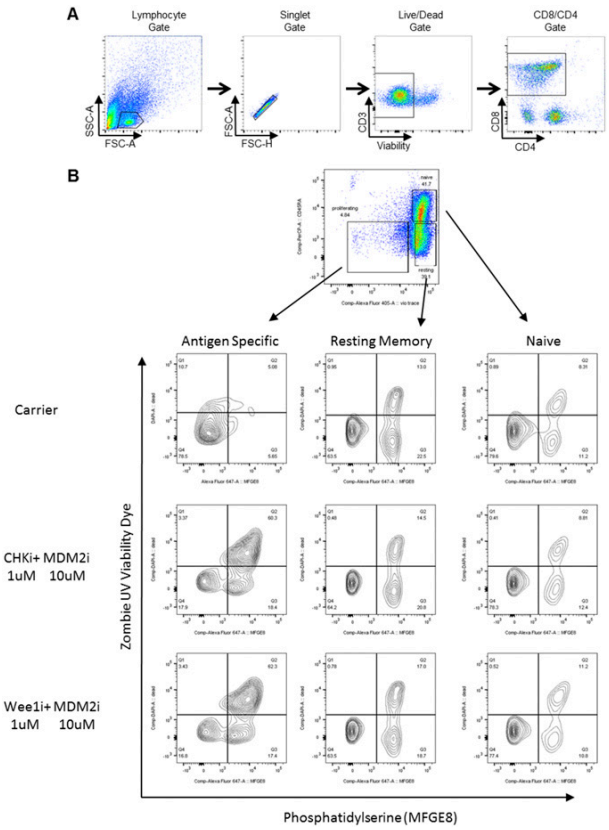

Fig. S5. Gating strategies/representative dot plots. (*A*) Gating for data in Fig. 8*C*: PBMCs from healthy donors or patients with untreated HLH. (*B*) Related to Fig. 9 *D*–*F*: Human T cells were activated from healthy donor PBMCs with a CMV peptide pool followed by IL-2 for a total of 6 d. Representative flow plots and gating strategy are shown for antigen-specific, resting memory, and naive T cells cultured with the indicated treatments (5 μM $MDM2_i$, 3 μM etoposide, 1 μM CHK_i, and 1 μM $WEE1_i$). Apoptosis was determined by viability dye and phosphatidylserine (PS) staining after 18 h.